Hindawi
International Journal of Antennas and Propagation
Volume 2021, Article ID 8022207, 10 pages
https://doi.org/10.1155/2021/8022207

Research Article

Dual Circularly Polarized Patch Antenna with Improved Interport Isolation for S-Band Satellite Communication

Haq Nawaz,[1] **Ahmad Umar Niazi**,[2] **and Mansoor Ahmad**[3]

[1]*Electrical Engineering, University of Engineering and Technology (UET), Lahore, Pakistan*
[2]*Electronics Engineering, University of Engineering and Technology (UET), Taxila, Pakistan*
[3]*Department of Electronics, University of Buner, Buner, Khyber Pakhtunkhwa, Pakistan*

Correspondence should be addressed to Haq Nawaz; hnawaz@sabanciuniv.edu

Received 25 May 2021; Revised 12 August 2021; Accepted 3 September 2021; Published 17 September 2021

Academic Editor: Ahmad Safaai-Jazi

This paper presents a bi-port, single-layered (planar), dual circularly polarized (CP) patch antenna with improved interport isolation for S-band satellite telemetry and telecommand applications. The dual-port, planar antenna is based on a square-shaped radiator with trimmed corner to achieve CP characteristics (RHCP and LHCP) for excitations from respective ports. However, the RF isolation between the two ports is very low due to strong power leakage from transmit (T_x) to transmit (R_x) port. The externally employed tunable self-interference cancellation (SIC) circuit achieves high isolation between orthogonal ports while axial ratio (AR) is ≤3 dB for both right and left handed circular polarization modes. The employed single-tap SIC circuit/loop attains the high interport isolation through signal inversion mechanism. The proposed antenna design achieves ≥72 dB peak interport isolation in addition to ≥30 dB and 15 dB port to port isolation over the isolation or SIC bandwidths of 15 MHz and 90 MHz (−10 dB bandwidth for both ports), respectively. The port to port isolation performance is improved without significant degradation in antenna radiation characteristics. The validation model of the presented planar antenna based on single element characterizes much better measured interport isolation performance compared to those dual CP printed antennas reported earlier as endorsed through detailed comparison

1. Introduction

In order to eliminate the requirements of polarization alignment of satellite space link antennas, dual circular polarized radiators are deployed to feed dish-type satellite communication terminal antennas [1, 2]. Such circular polarized (CP) antennas in the satellite communication applications offer flexible orientations of the transmitter and receiver antennas [3]. The dual CP antennas can also play a vital role to minimize the fading loss and can be utilized for frequency reuse applications. Normally, dual CP waveguide horns are deployed as feeds for satellite dish antennas. However, dual CP microstrip patch antennas can be very useful as feeds for such applications as they can offer a low profile, easy manufacturing, conformability, and convenient integration with other RF blocks in transmit and receive chains. Such dual CP microstrip antennas can also act as useful building blocks for aperture and feeds arrays in satellite communications.

The interport isolation is the deciding parameter to determine the viability of dual CP microstrip (planar) antennas for satellite communication applications. The overall system noise temperature or noise figure is highly dependent on the interport coupling of feed antennas [4]. For instance, in receive mode operation, the high mutual coupling between antenna's ports will increase the equivalent noise temperature of the receiver at satellite ground terminal. Thus, using a dual CP feed antenna with low or poor interport isolation will degrade the system sensitivity through direct contribution of additional noise.

However, it is very difficult and challenging task to achieve the high interport isolation for shared aperture (radiator) antenna with dual CP characteristics due to presence of both vertical and horizontal electric field

components in each CP mode (RHCP and LHCP). The previously reported works on dual-port antennas with linear co-polarized characteristics have focused on suppression of interport coupling through signal inversion-based cancellation circuits [5] or balanced receive mode operation [6] to achieve high interport isolation for antennas with linear co-polarized characteristics. The combination of the signal inversion and differential receive mode technique offers nice interport isolation for such linear co-polarized antennas [5]. However, the differential feeding-based isolation technique is not viable for shared aperture trimmed corner CP antennas.

In this paper, a planar, squared-shaped radiating element was utilized with single corner trimming or truncation to produce dual CP characteristics when excited from the respective orthogonal ports. The single-layer antenna structure avoids multilayered complex printed circuit board (PCB) or stacked structures which are employed in conventional dual CP antennas. The improved interport isolation is achieved through a signal inversion-based decoupling network between orthogonal ports of CP element. The single-tap decoupling network is composed of two 3 dB couplers, a tunable phase shifter, and voltage controlled attenuator. The tunable self-interference cancellation (SIC) circuit also offers the possibility of setting the peak isolation at intended frequency within antenna's impedance bandwidth.

The rest of the paper is organized as follows. Section 2 details the design and simulated characteristics of a dual-port, dual circularly polarized antenna based on single square-shaped element with trimmed corner. Section 3 presents the design, simulations, and analysis of dual CP antenna with integrated single-tap SIC loop to achieve improved isolation between T_x and R_x ports. The implementation details and measurement results for the antenna with integrated SIC circuit are presented in Section 4. The conclusions are drawn in Section 5.

2. Two-Port, Dual Circularly Polarized Antenna Element

The proposed dual CP antenna is based on a square-shaped radiating element with two orthogonal feeds as shown in Figure 1. The dual CP characteristics were obtained through proper corner trimming or truncation when patch is excited from respective orthogonally placed ports. The antenna was designed on 1.6 mm thick FR4 substrate ($\varepsilon_r = 4.4$, $\tan\delta = 0.02$).

The proposed dual CP antenna is simulated by using Keysight Advanced Design System (ADS) and HFSS software [7]. The corner-trimmed mechanism generates two orthogonal E-field components with equal magnitude and 90° phase difference when patch is excited through respective port to produce CP characteristics as illustrated in Figure 2. The proposed antenna will be right-hand circular polarized (RHCP) when port 1 is excited, and similarly, it is left-hand circular polarized (LHCP) for port 2 excitation. The corner truncation topology offers the advantage to implement CP antenna on single-layered PCB (radiating element and feeds on same side of PCB) as compared to other feeding configurations including cross-slot fed, circularly polarized patches [8] based on three-layered stacked structure.

The simulated reflection coefficients (S_{11}, S_{22}) and interport coupling (S_{21}) results for proposed bi-port, dual CP antenna are shown in Figure 3. The 10 dB return loss bandwidth for proposed dual port, dual CP antenna is better than 75 MHz for each port as clear from simulation results. As expected and clear from simulated interport coupling results, both ports of dual CP patch antenna are not well isolated as the isolation levels are around 8 dB only.

Ansys HFSS simulated peak realized gain and axial ratio results for proposed corner-trimmed, CP antenna are given in Figure 4. For brevity, only the simulated results for port 1 excitation (RHCP mode) are presented here. Due to symmetry of proposed antenna structure, the simulated peak realized gain and axial ratio results for port 2 (LHCP) will be identical to those observed for RHCP mode. As clear from simulation results in Figure 4, the proposed CP antenna achieves axial ratio (AR) ≤1 dB with simulated peak realized gain of better than 4.8 dBi at centre design frequency of 2.4 GHz. Moreover, as clear from AR versus theta simulation results in Figure 5, the antenna achieves a wider 3 dB AR beamwidth.

Ansys HFSS simulated gain versus theta results for different phi cuts (at $\Phi = 0°$, 45°, and 90°) are shown in Figure 6 for RHCP mode (port 1 excitation). The simulated boresight gain is around 4.7 dBi for all three Φ cuts. These simulated gain results demonstrate the good CP characteristics of antenna as it provides almost same gain levels at different values of phi (Φ). The gain of the proposed dual CP antenna can be enhanced by using a low loss substrate which will improve the radiation efficiency of printed patch to offer more gain levels.

3. Dual Circularly Polarized Antenna with SIC Circuit for Improved Isolation

After validating the radiation characteristics of proposed antenna, the interport isolation of dual-port, dual CP antenna presented in Section 2 was improved by using an external SIC circuit between port 1 and port 2. The external SIC circuit is composed of two 3 dB couplers, a tunable RF attenuator, and voltage controlled phase shifter as illustrated in Figure 7. 3 dB coupler 1 placed at port 1 is used to tap a RF signal to add its modified version at port 2 through coupler 2. The tunable phase shifter and attenuator are used to achieve required signal inversion conditions for T_x signals [5]. These signal inversion conditions require that RF signals from each path (through antenna and SIC network) should be equal in magnitude and 180° out of phase when they are combined at port 2 for cancellation. As stated earlier in Figure 3, the antenna interport coupling is around −8 dB which requires same levels of coupling through SIC network along with 180° phase difference between these two signals.

The interport isolation improvement capabilities of SIC circuit with dual CP antenna were endorsed through co-simulations in Keysight ADS software. The co-simulation schematic is shown in Figure 8, where the EM model of bi-

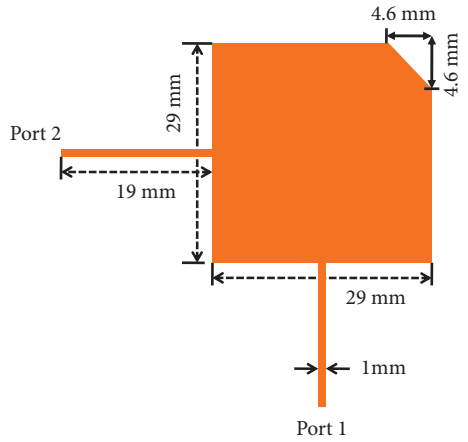

Figure 1: The proposed corner-trimmed, dual CP, 2.4 GHz patch antenna.

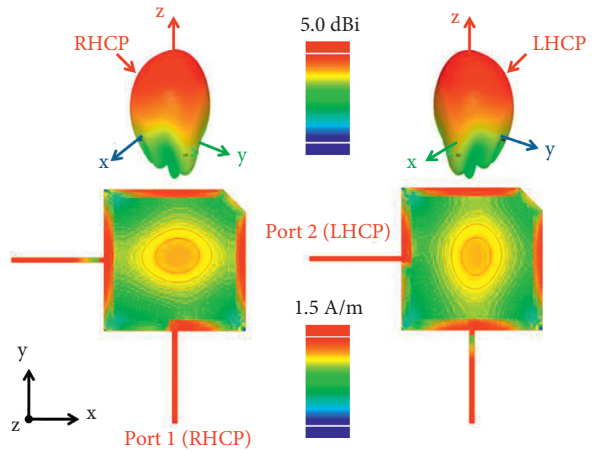

Figure 2: The simulated surface current distributions and gain patterns for RHCP and LHCP characteristics of the proposed dual CP antenna at $f = 2.4$ GHz.

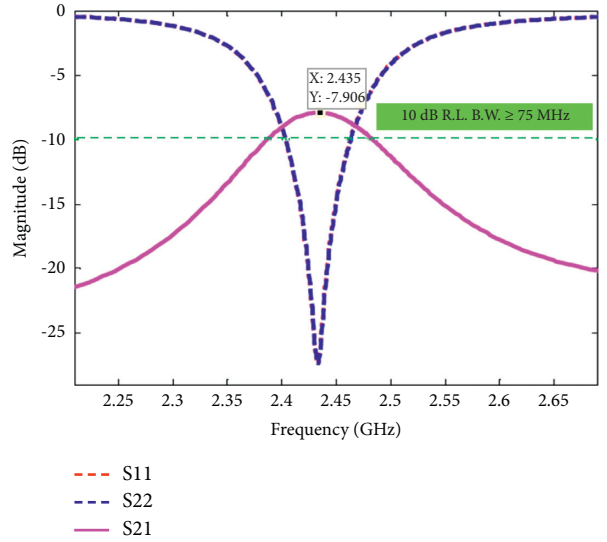

Figure 3: The simulated reflection coefficients (S_{11}, S_{22}) and interport coupling (S_{21}) results for proposed dual-port, dual CP patch antenna.

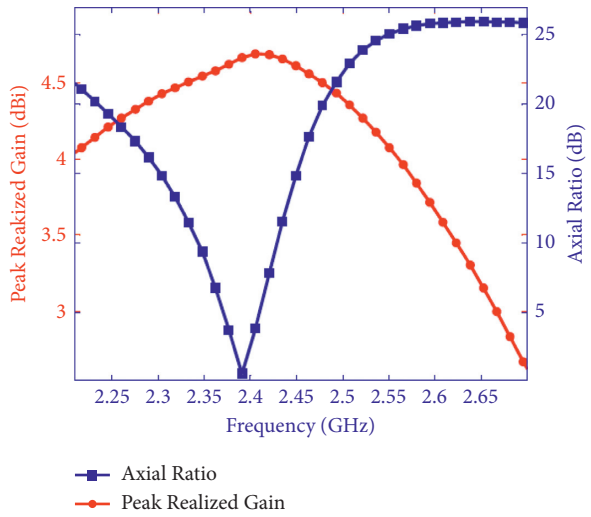

Figure 4: The simulated axial ratio and peak realized gain results for the dual-port, dual CP antenna when excited for RHCP mode (port 1).

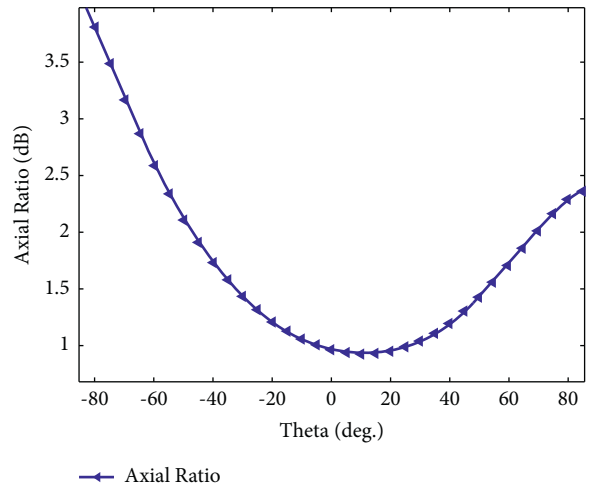

Figure 5: The simulated axial ratio versus theta results for proposed dual-port, dual CP antenna when excited for RHCP mode (port 1 excitation).

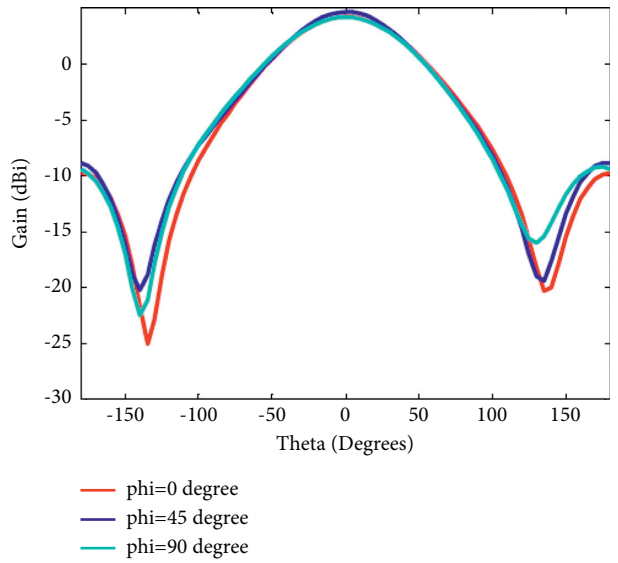

Figure 6: The simulated gain versus theta results at $\Phi = 0^\circ$, 45°, and 90° cuts for dual-port, dual CP antenna excited for RHCP mode (port 1 excitation).

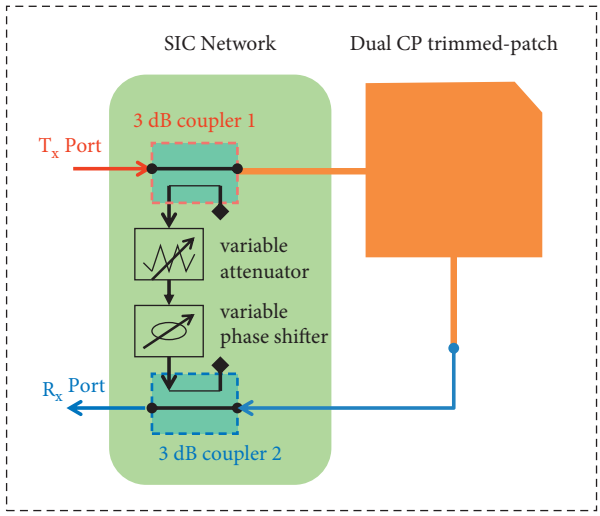

Figure 7: The dual CP trimmed-corner planar antenna with single-tap network/loop for improved interport isolation through SI suppression at R_x port.

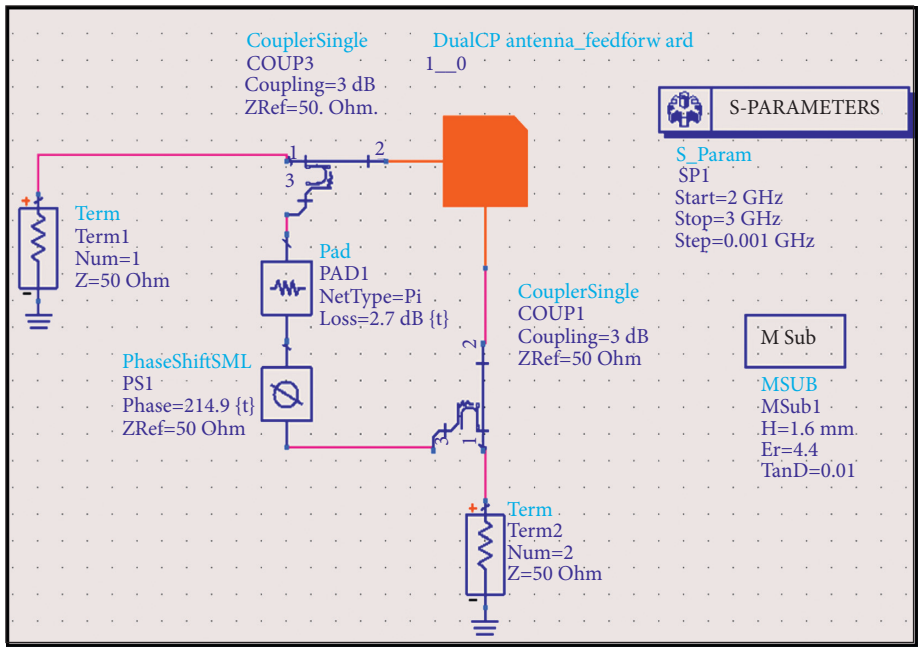

Figure 8: The schematic for co-simulation of dual CP antenna with SIC circuit.

port, dual CP antenna was used in schematic simulations. The phase shifter and attenuator in SIC loop were tuned to set the required SIC conditions to achieve the high isolation between port 1 and port 2. The simulation results are presented in Figure 9 where the interport isolation performance results for dual CP antenna with and without SIC circuit are presented for the comparison.

As clear from Figure 9, the peak isolation was ≥73 dB at 2.43 GHz frequency as compared to ~8 dB when no SIC circuit was used. Thus, more than 65 dB improvement in peak isolation is contributed by SIC circuit. Moreover, the simulated isolation was ≥30 dB and 18 dB within 20 MHz and 100 MHz bandwidths, respectively, as clearly indicated for results in Figure 9.

It is important to mention here that SIC capabilities of external circuit are highly sensitive to phase and attenuation variations of phase shifter and attenuator in the SIC loop as such variations will directly disturb the intended signal inversion conditions. The SIC circuit has the ability to tune out or suppress the interport isolation degradation resulting from environmental reflections in real-time deployment scenarios of proposed dual CP antenna [5]. The proposed SIC mechanism provides narrow band isolation performance as the single-tap SIC circuit has the limitation of setting signal inversion SIC conditions ideally for single frequency only. However, two-tap SIC circuits can provide comparatively wideband isolation or SIC performance as demonstrated in [9].

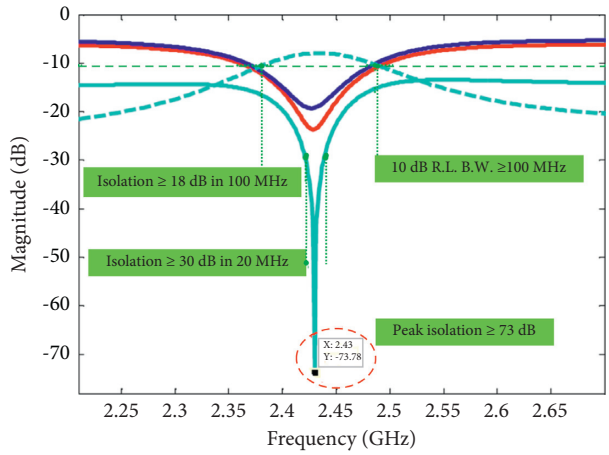

FIGURE 9: The simulated S_{11}, S_{22}, and S_{12} results for dual-port, dual CP patch antenna with external SIC circuit to achieve the improved interport isolation.

The tunable SIC circuit can be used to set the peak isolation notch frequency through variations in attenuation and phase to set SIC conditions for intended frequency. In other words, any frequency with peak isolation can be achieved within required impedance bandwidth of dual CP antenna. Three example cases are presented here through simulation as shown in Figure 10. The SIC circuit is tuned to achieve ≥70 dB interport isolation at 2.4 GHz, 2.43 GHz, and 2.46 GHz frequencies as illustrated in Figure 10. Consequently, the SIC bandwidth can also be adjusted as per requirements of wireless communication link. For instance, the 20 MHz SIC band with ≥30 dB isolation is 2.39 GHz to 2.41 GHz for the case of peak isolation notch frequency of 2.4 GHz. Similarly, it is 2.45 GHz to 2.47 GHz for the case of the peak isolation notch frequency tuned at 2.46 GHz.

4. Prototype of Antenna with Integrated Single-Tap SIC Circuit

The validation model or prototype of the bi-port, dual CP printed antenna with integrated single-tap SIC network is depicted in Figure 11. The complete structure was implemented on 1.6 mm thick single-layered FR4 substrate with $\varepsilon_r = 4.4$ and $\tan\delta = 0.02$. As indicated in Figure 11, both 3 dB directional couplers are based on microstrip coupled line topologies. The coupled ports of these directional couplers are intended for tapping of RF signals from respective ports, as shown in Figure 11. The SMD versions of JSPHS-2484+ and EVA-3000+ from mini-circuits are utilized as variable phase shifter and attenuator, respectively. The EVA-3000+ variable attenuator offers typical attenuation variations of 3.5 dB to 24 dB for the tuning voltage range of 8 V to 0 V, while the JSPHS-2484+ variable phase shifter can offer the phase variations of 0° to 180° when the tuning voltage is varied from 0 to 15 Vdc.

The validation model of the presented antenna was characterized through experimentation in lab environment where the reflections from surroundings may result in severe degradation of interport isolation performance of such antennas. However, the employed SIC network offers capabilities to achieve high interport isolation even in the presence of such environmental reflections. The interport isolation characteristics of implemented antenna were recorded through tuning of variable attenuator and phase shifter for setting the loop attenuation and phase values to establish the required SIC conditions. The tuning in this fashion will achieve the optimum isolation levels at required resonating frequency of trimmed-corner patch as discussed earlier. The measured S_{11}, S_{22}, and S_{12} results for dual-port, dual CP antenna with integrated SIC network are presented in Figure 12. As clear from measured results in Figure 12, the peak isolation exceeds 72 dB at 2.45 GHz frequency for the validation model of antenna integrated with single-tap SIC network as compared to around 8 dB isolation for the case of antenna with no SIC circuit. Moreover, the recorded isolation levels ≥30 dB and 15 dB across the SIC bandwidths of 15 MHz and 90 MHz, respectively.

The measured peak gains and axial ratio versus frequency results for both RHCP and LHCP modes of validation model of dual-port trimmed corner patch integrated with SIC network are shown in Figure 13. As clear from these measurements, the peak gain is better than 4.5 dB for both RHCP and LHCP modes where each mode is excited through respective port of the antenna prototype (Figure 11). The measured gain levels are higher than 4.3 dB over the entire operating bandwidth of the antenna. This indicates that no significant degradation in radiation performance is resulting when the SIC network is used between two ports for improved interport isolation performance of presented dual-port patch antenna. Moreover, the measurement results of axial ratio versus frequency for antenna prototype indicate better than 3.5 dB axial ratio over the entire impedance bandwidth of the implemented dual CP antenna.

The experimental results of axial ratio versus elevation angle (theta) for excitation of both ports (RHCP and LHCP modes) of presented antenna's prototype are given in Figure 14. The presented dual-port, dual CP antenna offers very wide 3 dB axial ratio beamwidth in the elevation plane as clearly endorsed by the measurement results shown in Figure 14.

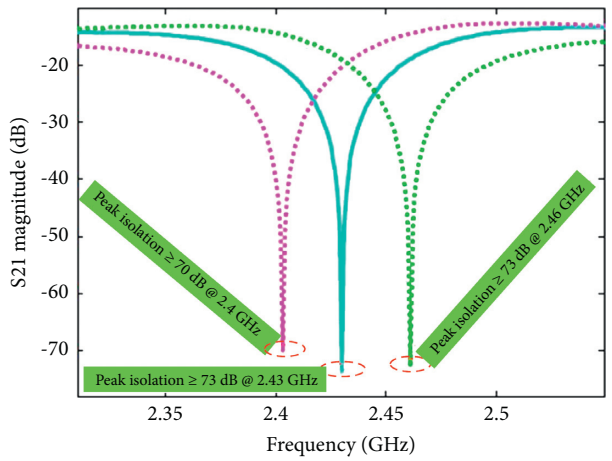

Figure 10: The simulated interport isolation results for three cases of peak isolation notch frequencies tuned at 2.4 GHz, 2.43 GHz, and 2.46 GHz.

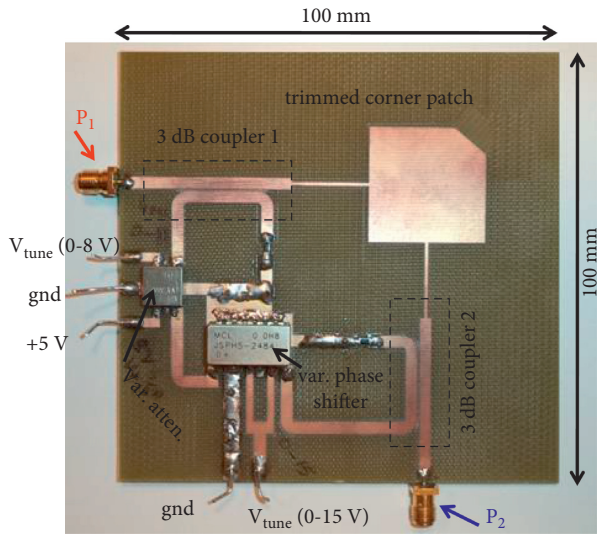

Figure 11: The validation model or prototype of dual CP antenna with integrated SIC circuit.

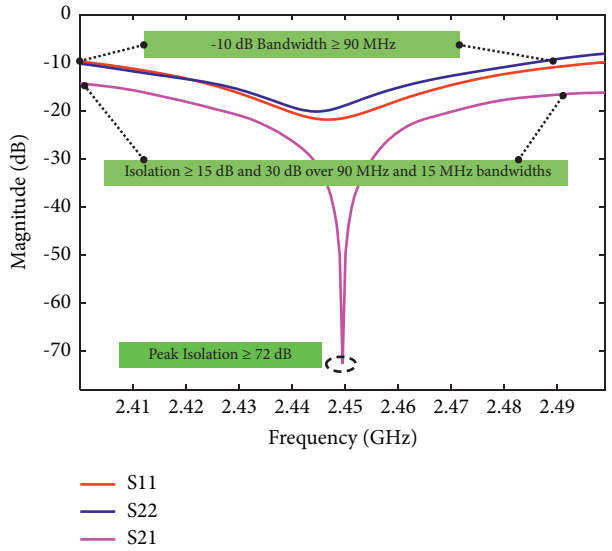

Figure 12: The measured S_{11}, S_{22}, and S_{12} results for dual-port, dual CP patch antenna with integrated SIC network to achieve improved isolation.

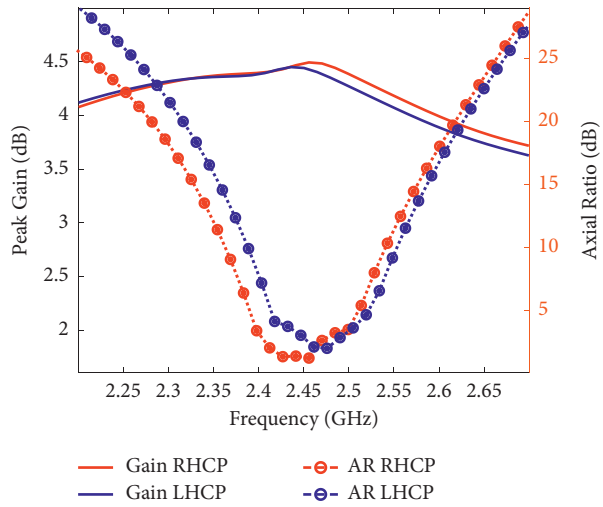

Figure 13: The measured peak gain and axial ratio versus frequency results for both modes of dual-port, dual CP antenna with integrated SIC network.

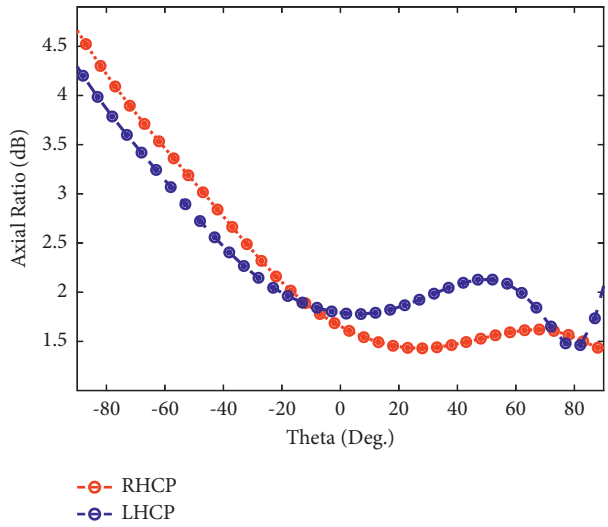

Figure 14: The measured axial ratio versus theta results for validation model of dual-port, dual CP antenna with integrated SIC network.

The measured 2D radiation patterns for co- and cross-polarization levels versus theta for the prototype of dual-port, dual CP antenna are given in Figure 15 for both RHCP and LHCP modes. The measured gain levels are higher than 4.5 dB at boresight for each of the intended polarizations. Moreover, the cross-polarization levels are more than 20 dB lower than the respective co-polarization levels which indicate the excellent polarization purity for both modes.

As detailed in Table 1, the interport isolation characteristics of our presented antenna have been compared to some previously reported designs of dual CP antennas. Both dual CP antennas reported in [1, 3] have achieved maximum isolation of 23 dB and 15.7 dB, respectively, for Ku-band applications. As compared to these two antennas, our proposed antenna offers ≥72 dB peak isolation for S-band applications. Moreover, it is important to note that low interport isolation levels are inherent in dual-port, dual CP patch antennas at low frequencies [22]. The dual-band (S and C bands), dual CP antenna reported in [10] is based on complex five-layered stacked structure. The measured peak isolation for this antenna is ~9 dB and 10 dB, and return loss bandwidth is around 150 MHz for low-frequency band (S-band). For high band (C-band), the measured peak isolation is ~27 dB and measured return loss ≥10 dB for both ports. Again our proposed antenna is based on low profile planar structure and offers better interport isolation performance for S-band applications.

The compact dual-band circular polarized antenna reported in [11] offers the measured average isolation levels of 5.8 dB and 5 dB for band 1 and band 2, respectively. Moreover, the structure is composed of a pentagonal radiator and a stacked rectangular parasitic element. The dual circularly polarized (DCP) microstrip antenna presented in [12] achieves impedance bandwidth of 399 MHz for C-band applications. The port to port isolation is more than 30.8 dB in the entire band with maximum isolation of 59.4 dB.

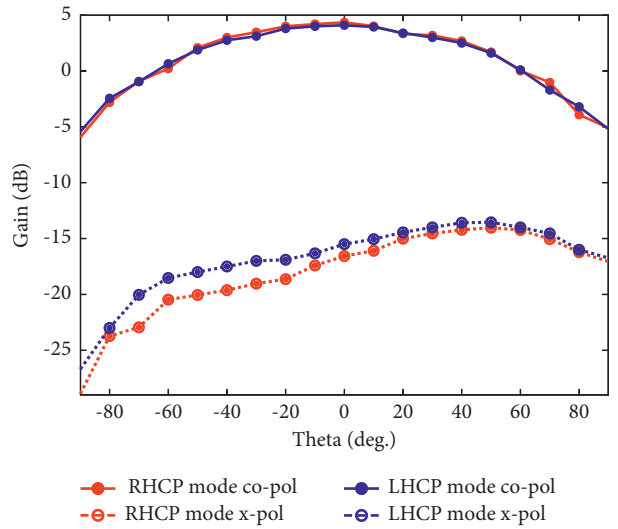

Figure 15: The measured 2D radiation patterns for co- and cross-polarization levels versus theta for prototype of dual-port, dual CP antenna with integrated SIC network.

Table 1: The comparison of isolation performance of presented antenna with previously reported bi-port, dual circularly polarized antennas.

Ref. designs	Peak isolation	−10 dB bandwidth
[1]	23 dB	Not stated
[3]	15.7 dB	Not stated
[10] (low band)	10 dB	~150 MHz
[10] (high band)	~27 dB	–
[11] (band 1)	Average isolation = 5.8 dB	380 MHz
[11] (band 2)	Average isolation = 5.0 dB	770 MHz
[12]	~60 dB	399 MHz
[13]	≥15.2 dB	50 MHz
[14]	35 dB	200 MHz
[15]	45 dB	1500 MHz
[16]	50 dB	85 MHz
[17]	36 dB	1340 MHz
[18]	20 dB	300 MHz
[19]	20 dB	150 MHz
[20]	45 dB	80 MHz
[21]	25 dB	900 MHz
This work	**72 dB**	**90 MHz**

Although the reported antennas in [11, 12] have achieved more impedance bandwidths compared to our proposed antenna, the peak isolation performance of our antenna is much better than that of both antennas. The DCP antenna based on the field transformation (FT) method is presented and reported in [13]. For this antenna, the recorded interport isolation is 15.2 dB at 2.42 GHz. Our proposed DCP antenna offers more impedance bandwidth and peak isolation compared to those achieved by antenna in [13]. Similarly, the peak interport isolation performance of our antenna is much better than designs reported in [14–21].

The proposed dual CP antenna with high interport isolation can be used in single (monostatic) antenna-based transceiver architecture to realize single-channel full-duplex or in-band full-duplex (IBFD) communication. For such applications, dual CP characteristics of RF signals in forward and reverse links will offer propagation domain isolation for two-way wireless communication links. For instance, for forward link, transceiver 1 will transmit with RHCP and transceiver 2 receives with RHCP. Conversely, for reverse link, transceiver 2 will transmit with LHCP and transceiver 1 receives with LHCP. For such configuration, both links are isolated in propagation domain through polarization diversity.

5. Conclusion

A single-layered, trimmed corner, two-port, dual circularly polarized (CP) 2.4 GHz patch antenna has been presented where improved interport isolation has been achieved through externally employed single-tap SIC circuit. The employed isolation technique is based on signal inversion mechanism to suppress the leakage from T_x port to R_x port. The presented dual CP antenna with high interport isolation

performance is an attractive solution to be used as feed antenna for S-band satellite dishes. Moreover, the design can be scaled accordingly to work at other satellite frequency bands. The isolation or SIC bandwidth of the presented antenna can be improved through two-tap SIC circuits, and the proposed antenna can be used effectively for 2.4 GHz in-band full-duplex wireless applications for simultaneous in-band transmit and receive operation. This will offer improved spectral efficiency or throughput compared to conventional time division and frequency division duplexing techniques for bidirectional wireless communication links. Moreover, the gain of the antenna can be enhanced through improvement in radiation efficiency by using some substrate with low loss. For instance, as stated in [22], the radiation efficiency is improved from 50% to 88% for $\tan\delta$ is reduced from 0.02 to 0.001. This will offer approximately 3 dB additional gain for the proposed antenna. Such low loss substrate will result in minor reduction in impedance bandwidth of proposed dual CP antenna. Moreover, the proposed antenna can be deployed in array configuration to achieve high gain levels.

Data Availability

The data used to support the design and validation of the presented antenna are available from the corresponding author upon request.

Conflicts of Interest

The authors declare that they have no conflicts of interest.

References

[1] M. Khan and K. F. Warnick, "Noise figure reduction by port decoupling for dual circular polarised microstrip antenna," *Electronics Letters*, vol. 50, no. 23, pp. 1662–1664, 2014.

[2] S. A. Rezaeieh, "Dual band dual sense circularly polarised monopole antenna for GPS and WLAN applications," *Electronics Letters*, vol. 47, no. 22, pp. 1212–1214, 2011.

[3] M. Khan, Z. Yang, and K. Warnick, "Dual-circular-polarized high-efficiency antenna for ku-band satellite communication," *IEEE Antennas and Wireless Propagation Letters*, vol. 13, pp. 1624–1627, 2014.

[4] K. F. Warnick, B. Woestenburg, L. Belostotski, and P. Russer, "Minimizing the noise penalty due to mutual coupling for a receiving array," *IEEE Transactions on Antennas and Propagation*, vol. 57, no. 6, pp. 1634–1644, 2009.

[5] H. Nawaz, Ö. Gürbüz, and I. Tekin, "Co-polarized monostatic antenna with high Tx-Rx isolation for 2.40 GHz single channel full duplex applications," *Microwave and Optical Technology Letters*, vol. 61, no. 4, pp. 1065–1069, 2019.

[6] H. Nawaz and I. Tekin, "Three ports microstrip patch antenna with dual linear and linear co-polarisation characteristics," *Electronics Letters*, vol. 53, no. 8, pp. 518–520, 2017.

[7] http://edadocs.software.keysight.com/display/ads2011/Setting+up+Momentum+Simulations.

[8] J. Wu, M. Li, and N. Behdad, "A wideband, unidirectional circularly polarized antenna for full-duplex applications," *IEEE Transactions on Antennas and Propagation*, vol. 66, no. 3, pp. 1559–1563, 2018.

[9] H. Nawaz, Ö. Gürbüz, and I. Tekin, "2.4 GHz dual polarised monostatic antenna with simple two-tap RF self-interference cancellation (RF-SIC) circuitry," *Electronics Letters*, vol. 55, no. 6, pp. 299-300, 2019.

[10] W. M. Dorsey and A. I. Zaghloul, "Dual-band, dual-circularly polarised antenna element," *IET Microwaves, Antennas & Propagation*, vol. 7, no. 4, pp. 283–290, 2013.

[11] T. Alam and M. T. Islam, "A dual-band Antenna with dual-circular polarization for nanosatellite payload application," *IEEE Access*, vol. 6, pp. 78521–78529, 2018.

[12] S. Chaudhuri, R. S. Kshetrimayum, and R. K. Sonkar, "High inter-port isolation modified Franklin dual circularly polarized microstrip antenna," in *Proceedings of the European Conference on Antennas and Propagation (EuCAP)*, Krakaw, Poland, March 2019.

[13] H. Shi, H. Giddens, and Y. Hao, "Dual-circularly polarized patch antenna using field transformation medium," *IEEE Antennas and Wireless Propagation Letters*, vol. 16, pp. 2869–2872, 2017.

[14] X.-Z. Lai, Z.-M. Xie, and X.-L. Cen, "Design of dual circularly polarized antenna with high isolation for rfid application," *Progress In Electromagnetics Research*, vol. 139, pp. 25–39, 2013.

[15] S. Liu, D. Yang, and J. Pan, "A low-profile broadband dual-circularly-polarized metasurface antenna," *IEEE Antennas and Wireless Propagation Letters*, vol. 18, no. 7, pp. 1395–1399, 2019.

[16] E. Zhang, A. Michel, M. R. Pino, P. Nepa, and J. Qiu, "A dual circularly polarized patch antenna with high isolation for MIMO WLAN applications," *IEEE Access*, vol. 8, pp. 117833–117840, 2020.

[17] S. Chaudhuri, R. S. Kshetrimayum, and R. K. Sonkar, "High inter-port isolation dual circularly polarized slot antenna with split-ring resonator based novel metasurface," *AEU-International Journal of Electronics and Communications*, vol. 107, pp. 146–156, 2019.

[18] R. Ferreira, J. Joubert, and J. W. Odendaal, "A compact dual-circularly polarized cavity-backed ring-slot antenna," *IEEE Transactions on Antennas and Propagation*, vol. 65, no. 1, pp. 364–368, 2017.

[19] A. Narbudowicz, X. Bao, and M. J. Ammann, "Dual circularly-polarized patch antenna using even and odd feed-line modes," *IEEE Transactions on Antennas and Propagation*, vol. 61, no. 9, pp. 4828–4831, 2013.

[20] X.-Z. Lai, Z.-M. Xie, Q.-Q. Xie, and X.-L. Cen, "A dual circularly polarized RFID reader antenna with wideband isolation," *IEEE Antennas and Wireless Propagation Letters*, vol. 12, pp. 1630–1633, 2013.

[21] H. H. Tran, N. Nguyen-Trong, and H. C. Park, "A compact dual circularly polarized antenna with wideband operation and high isolation," *IEEE Access*, vol. 8, pp. 182959–182965, 2020.

[22] R. P. Owens and A. C. Smith, "Low-profile dual band, dual polarised array antenna module," *Electronics Letters*, vol. 26, no. 18, pp. 1433-1434, 1990.